Calhoun: The NPS Institutional Archive

2013

Comb-based radio-frequency photonic filtering with 20 ns bandwidth reconfiguration

Wu, Rui

http://hdl.handle.net/10945/52403

Comb-based radio-frequency photonic filtering with 20 ns bandwidth reconfiguration

Rui Wu,* Minhyup Song, Daniel E. Leaird, and Andrew M. Weiner

School of Electrical and Computer Engineering, Purdue University, 465 Northwestern Avenue,
West Lafayette, Indiana 47907-2035, USA
*Corresponding author: rwu@purdue.edu

We present a scheme to generate a 10 GHz optical frequency comb that is bandwidth reconfigurable on a time scale of tens of nanoseconds via electronic control of the drive signal to a phase modulator. When such a comb is used as the source for a radio-frequency (RF) photonic filter employing dispersive propagation, the RF filter bandwidth varies in inverse proportion to the optical bandwidth. As a result we are able to demonstrate, for the first time to our knowledge, bandwidth-reconfigurable RF filtering with transition times under 20 ns. The reconfiguration speed is determined by the response time of a programmable RF variable attenuator. © 2013 Optical Society of America

OCIS codes: (060.5625) Radio frequency photonics; (120.2440) Filters; (230.2090) Electro-optical devices.
http://dx.doi.org/10.1364/OL.38.002735

Radio-frequency (RF) photonic filters have received sustained research attention due to their potential for broad band tuning, reconfigurability, immunity to electromagnetic interference, and compatibility with remote fiber optic connections [1–5]. High-repetition-rate optical frequency combs have received great interest for many applications, including optical arbitrary waveform generation [6], coherent communication [7], short pulse generation [8–10], and recently microwave signal processing [4,5,11]. RF photonic filters based on high-repetition-rate frequency combs [4,5] have been demonstrated with high selectivity, with rapid tuning of the passband frequency, and with quasi-static RF bandwidth reconfigurability [5]. However, dynamic RF bandwidth reconfiguration was not considered. Although there has been much effort toward implementation of bandwidth-reconfigurable filters based on RF circuit approaches [12–16], to the best of our knowledge, rapid RF bandwidth reconfiguration (for example, at the level of tens of nanoseconds) has not been reported. Here we demonstrate an approach in which the optical bandwidth of an electro-optically generated frequency comb is rapidly changed through electronic control of the phase modulation index. When the comb is used as the source in an RF photonic filter configuration, the RF filter

bandwidth varies in inverse proportion to the optical bandwidth. As a result, we have demonstrated RF bandwidth reconfiguration with transition times under 20 ns while keeping the mainlobe-to-sidelobe suppression ratio (MSSR) larger than 30 dB. Figure 1 shows the experimental setup for our RF bandwidth-reconfigurable filter. The dotted part is the 10 GHz bandwidth-reconfigurable optical frequency comb generator, which is a sequence of lithium niobate electro-optic intensity and phase modulators. The modulator sequence is designed to generate an approximately Gaussian-shaped optical comb spectrum [5,10] based on time-to-frequency mapping theory [17–19]. We fix the RF power on one phase modulator to 30 dBm, while the RF power on the other phase modulator is electronically controlled via a variable attenuator (American Microwave Corporation, model no. SAB-2DR-30). The RF power to the second phase modulator is 30 dBm when the variable attenuator is switched off (minimal attenuation) and 7 dBm with the attenuator switched "ON" (23 dB attenuation). The comb bandwidth is proportional to the modulation index on the phase modulators [5,10]; hence in our scheme the optical bandwidth can be switched by nearly a factor of 2. For filtering applications, the generated comb is modulated with the RF input signal. Here we use a single-sideband
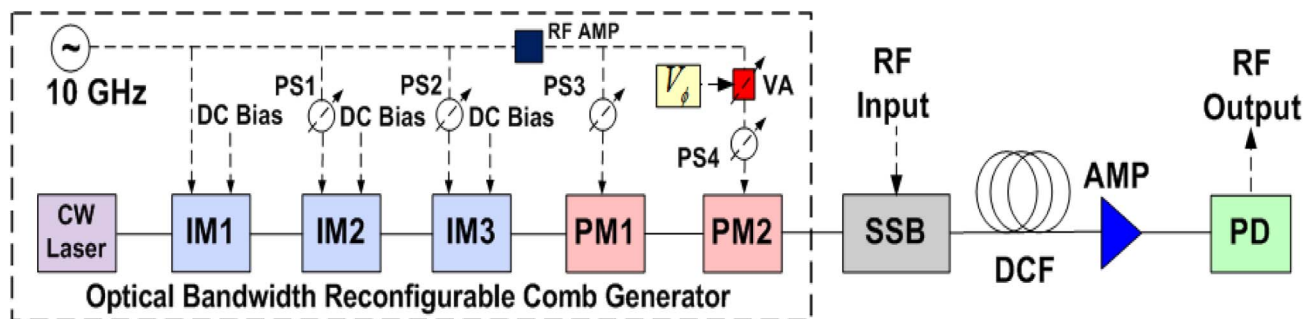

Fig. 1. Experimental scheme to implement bandwidth-reconfigurable RF photonics filtering based on optical bandwidth tunable optical frequency combs. CW, continuous wave; IM, intensity modulator; PM, phase modulator; PS, phase shifter; VA, RF variable attenuator; SSB, single-sideband modulator; DCF, dispersion-compensating fiber; AMP, optical amplifier; RF AMP, RF amplifier; PD, photodetector.

modulation format to avoid dispersive fading, as in [4]. (In a modified interferometric arrangement of the comb-based filter, double-sideband modulation may be used without dispersive fading effects [20].) Then the signal passes through a 6.7 km dispersion-compensating fiber (DCF) with specified dispersion of −247 psnm^{-1} km^{-1} at 1550 nm and is detected by a 20 GHz bandwidth photo-detector. Each line of the optical frequency comb acts as a distinct filter tap, with 126.58 ps tap delay between adjacent 10 GHz comb lines.

One advantage of comb-based microwave photonic filtering is that a large number of taps can be easily generated from a single continuous-wave (CW) laser and dispersive element. The filter transfer function can be written as [4,5]

$$H(\omega_{RF}) \propto \sum_{n=0}^{n=N-1} |e_n|^2 e^{jnD2\pi\Delta f \omega_{RF}}, \qquad (1)$$

where e_n is the complex electrical field of the nth comb line, D is the fiber dispersion, Δf is the repetition rate of the comb, $2\pi D\Delta f$ is the tap delay between two adjacent taps, and ω_{RF} is the microwave frequency. Equation (1) indicates that the RF bandwidth varies in inverse proportion to the bandwidth of the optical frequency comb, which is in turn proportional to the modulation index of the phase modulators.

Figure 2 shows an example of simulation results. Figures 2(a) and 2(b) show Gaussian apodized combs at 10 GHz repetition rate with 20 lines (102 GHz 3 dB bandwidth) and 36 lines (182 GHz 3 dB bandwidth), respectively. Since total optical power is not changed with phase modulation depth, the power at the peak of the comb spectrum in Fig. 2(b) is reduced compared to that in Fig. 2(a). Figure 2(c) shows the simulated filter transfer functions for combs from Figs. 2(a) and 2(b). A decrease in the 3 dB RF filter bandwidth from 513 MHz

(narrow comb) to 285 MHz (broad comb) is predicted. However, the amplitude of the response at the peak of the filter passbands does not change. Figure 3 shows experimental results, with optical spectra [Figs. 3(a) and 3(b)] measured using an optical spectrum analyzer (OSA) set at 0.01 nm resolution and the RF filter transfer function [Fig. 3(c)] measured using a vector network analyzer (VNA). By switching the variable attenuator from "ON" to "OFF", the optical 3 dB bandwidth increases from 0.82 to 1.62 nm. The resulting filter transfer function shown in Fig. 3(c) reveals a decrease in 3 dB bandwidth of the RF filter passband by nearly a factor of 2, from 518 to 272 MHz, similar to the simulation predictions.

We now demonstrate RF bandwidth reconfiguration by simultaneously injecting RF tones at 7.9 and 8.4 GHz. These frequencies [marked with vertical lines in Fig. 3(c)] are selected to emphasize the effect of changing the filter bandwidth. We intentionally set the power of the 8.4 GHz tone to be 8 dB larger at the input than that of the 7.9 GHz tone. This leads to equal RF output at both frequencies when the attenuator is switched on [Fig. 4(a)]. Figure 4(b) shows the corresponding oscilloscope trace of the filtered RF output, measured with a 50 Gsample/s real-time oscilloscope. The RF waveform exhibits strong modulation at the 500 MHz frequency difference of the input tones. When the attenuator is off, the narrower RF filter bandwidth results in attenuation of the 8.4 GHz output by >10 dB relative to the 7.9 GHz RF output [Fig. 4(c)]. Figure 4(d) shows the corresponding oscilloscope trace. Since the powers of the RF tones are now quite different, the 500 MHz modulation is largely suppressed in the time domain data of Fig. 4(d). These results confirm RF bandwidth configuration.

Figure 5 demonstrates fast RF bandwidth reconfiguration by applying a rapidly varying ON/OFF control
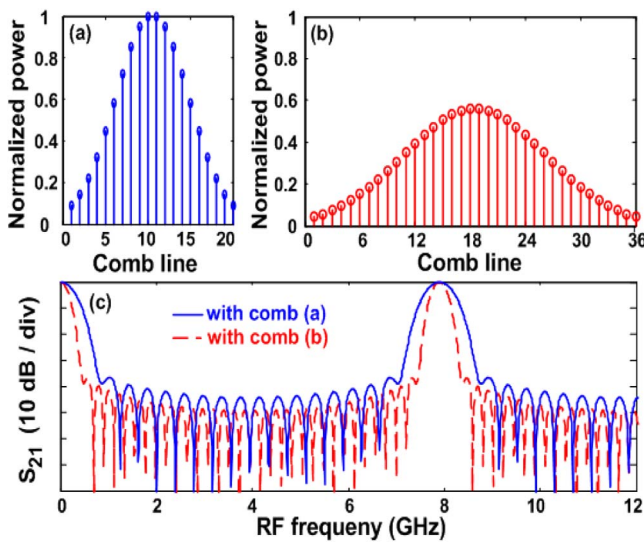

Fig. 2.   Simulation results of bandwidth-reconfigurable filter. (a) Optical frequency comb spectrum with 20 comb lines. (b) Optical frequency comb spectrum with 36 comb lines. (c) Calculated filter transfer functions with combs a and b, respectively.
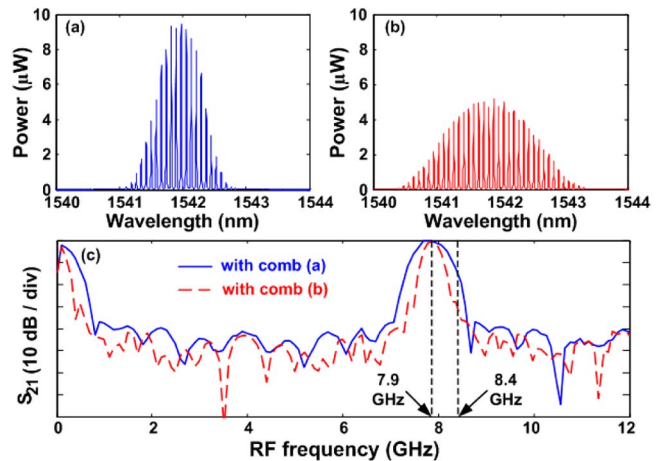

Fig. 3.   Experimental results of the bandwidth-reconfigurable RF photonic filtering through the use of a programmable RF variable attenuator. (a) Optical frequency comb spectrum with the variable attenuator switched "ON". (b) Optical frequency comb spectrum with the variable attenuator switched "OFF". (c) Measured RF filter transfer functions with comb a (attenuator switched "ON") and comb b (attenuator switched "OFF"). Nearly a factor of 2 change in RF bandwidth is observed.
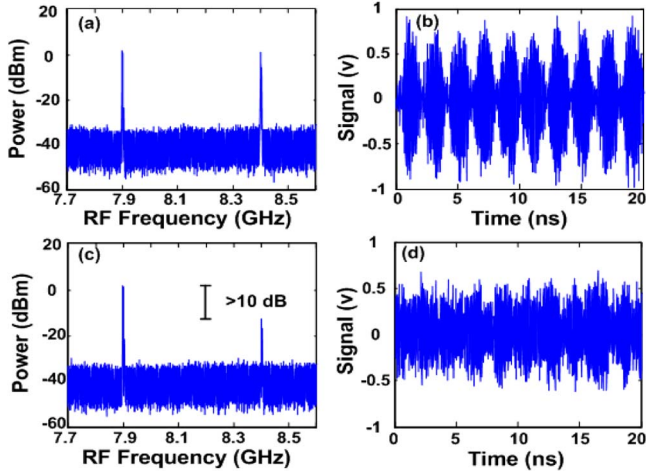
Fig. 4. Experimental characterization of RF bandwidth reconfiguration in both time and frequency domains by switching the attenuator "ON" and "OFF". Frequency domain data are obtained by using an RF spectrum analyzer. Time domain data are obtained by using a real-time oscilloscope. (a), (b) Switched "ON": (a) output RF spectrum showing the two RF frequency tones at 7.9 and 8.4 GHz have approximately equal power; (b) output time domain RF waveform. (c), (d) Switched "OFF": (c) output RF spectrum showing the two RF frequency tones at 7.9 and 8.4 GHz have >10 dB power difference; (d) output time domain RF waveform.

signal with 0.64 ns rise/fall time at 625 KHz modulation rate (1.6 μs period) to the variable attenuator. The oscilloscope trace of the filtered RF output is shown in Fig. 5(a). Close-ups of the waveform are shown for times corresponding to the attenuator switched off [Fig. 5(b)] and to the attenuator switched on [Fig. 5(c)]. These traces are similar to Figs. 4(d) and 4(b), respectively, which were obtained under quasi-static attenuator control. Figure 5(d) shows a spectrogram of the oscilloscope data in Fig. 5(a) calculated using a sliding fast Fourier transform Hamming window of 41 ns duration, providing an intuitive visual representation of the filter output. Examination of the rapid transitions at the rising and falling edges of the feature at 8.4 GHz [Figs. 5(e) and 5(f), respectively] reveals that the filter is able to reconfigure within 20 ns transition time, limited by the response time of the RF variable attenuator.

It is worth noting that filter reconfiguration occurs with a latency of 34 μs, not shown in Fig. 5, due to propagation delay in the dispersive fiber. This could be reduced to a time scale less than or equal to the reconfiguration time by replacing the dispersive fiber with a chirped fiber Bragg grating. It is also worth noting that the MSSR and stop-band attenuation (roughly 30 and 40 dB in current experiments) are set by the accuracy, in particular the smoothness, with which the Gaussian apodization of the optical power spectrum is achieved. In [10] we achieved 40 dB MSSR by adjusting the comb generation setup to produce a smoother Gaussian spectrum, while in [5] we achieved >60 dB MSSR and >70 dB stop-band attenuation though a nonlinear optics spectral smoothing scheme. In principle, these techniques should be compatible with the scheme introduced here, offering potential for simultaneous rapid bandwidth modulation and high filter contrast.
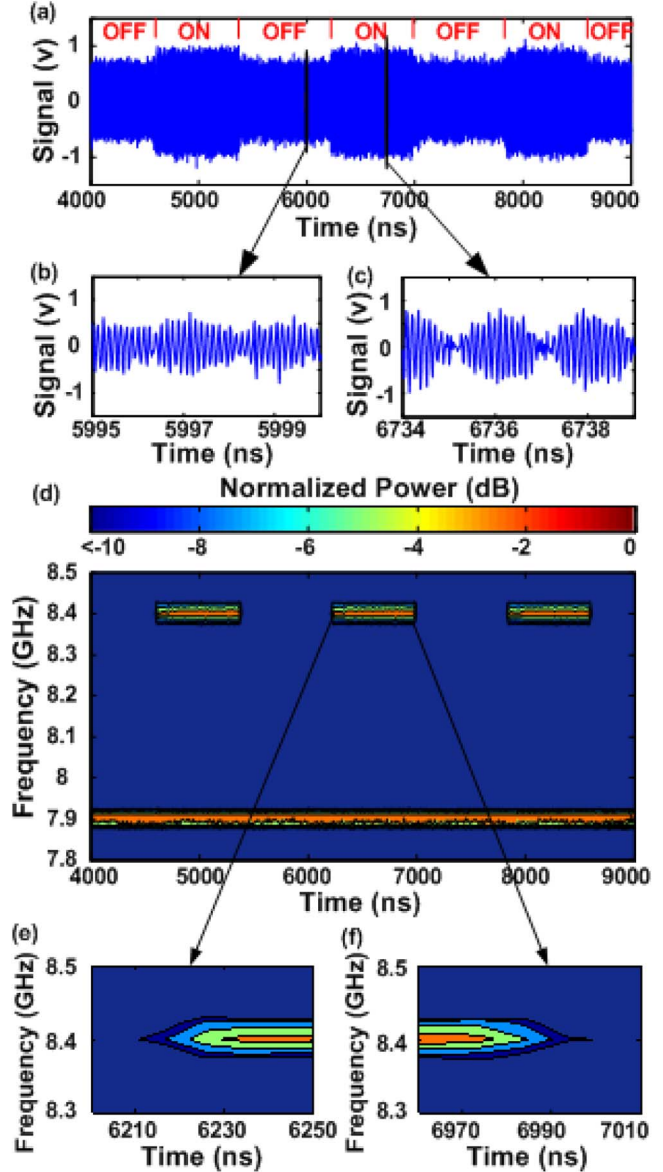

Fig. 5. Experimental results showing rapid RF bandwidth reconfigurability. (a) Measured oscilloscope signal at filter output. (b), (c) Close-ups of the output waveform with (b) attenuator "OFF" and (c) attenuator "ON". (d) Spectrogram representation of the output filtered signal. (e), (f) Close-ups of the spectrogram at (e) rising and (f) falling edges of the spectrogram feature at 8.4 GHz.

In summary, we have generated a 10 GHz optical frequency comb that is bandwidth reconfigurable on a time scale of tens of nanoseconds via electronic control of the phase modulation index. Using this comb as the optical source for RF photonic filtering experiments, we have demonstrated nearly a factor of 2 RF bandwidth reconfiguration within 20 ns. Our results clearly illustrate that the flexibility of electro-optically generated frequency combs provides substantial potential benefits for applications in RF photonic filtering.

References

1. A. J. Seeds and K. J. Williams, J. Lightwave Technol. **24**, 4628 (2006).
2. J. Capmany, B. Ortega, and D. Pastor, J. Lightwave Technol. **24**, 201 (2006).
3. J. Yao, J. Lightwave Technol. **27**, 314 (2009).
4. E. Hamidi, D. E. Leaird, and A. M. Weiner, IEEE Trans. Microwave Theory Tech. **58**, 3269 (2010).
5. V. R. Supradeepa, C. Long, R. Wu, F. Ferdous, E. Hamidi, D. Leaird, and A. M. Weiner, Nat. Photonics **6**, 186 (2012).
6. Z. Jiang, C. B. Huang, D. E. Leaird, and A. M. Weiner, Nat. Photonics **1**, 463 (2007).
7. A. D. Ellis and F. C. G. Gunning, IEEE Photon. Technol. Lett. **17**, 504 (2005).
8. I. Morohashi, T. Sakamoto, H. Sotobayashi, T. Kawanishi, and I. Hosako, Opt. Lett. **34**, 2297 (2009).
9. A. M. Clarke, D. G. Williams, M. A. F. Roelens, and B. J. Eggleton, IEEE Photon. Technol. Lett. **28**, 97 (2010).
10. R. Wu, C. M. Long, D. E. Leaird, and A. M. Weiner, IEEE Photon. Technol. Lett. **24**, 1484 (2012).
11. C.-B. Huang, D. E. Leaird, and A. M. Weiner, Opt. Lett. **32**, 3242 (2007).
12. M. Sánchez-Renedo, R. Gómez-Garcia, J. I. Alonso, and C. Briso-Rodriguez, IEEE Trans. Microwave Theory Tech. **53**, 191 (2005).
13. H. Joshi, H. H. Sigmarsson, S. Moon, D. Peroulis, and W. J. Chappell, in *IEEE MTT-S International Microwave Symposium Digest* (IEEE, 2009), pp. 629–632.
14. C. H. Kim and K. Chang, IEEE Trans. Microwave Theory Tech. **58**, 3936 (2010).
15. X. Huang, Q. Feng, and Q. Xiang, IEEE Trans. Microw. Wirel. Compon. Lett. **22**, 176 (2012).
16. A. Serrano, F. S. Correra, T. Vuong, and P. Ferrari, IEEE Trans. Microwave Theory Tech. **60**, 484 (2012).
17. V. Torres-Company, J. Lancis, and P. Andrés, Opt. Lett. **33**, 1822 (2008).
18. J. Azana, Opt. Commun. **217**, 205 (2003).
19. J. Howe and C. Xu, J. Lightwave Technol. **24**, 2649 (2006).
20. E. Hamidi, R. Wu, V. R. Supradeepa, C. M. Long, D. E. Leaird, and A. M. Weiner, "Tunable radio frequency photonic filter based on intensity modulation of optical combs," presented at the International Meeting on Microwave Photonics, Montreal, Quebec, Canada, October 5–9, 2010.